VCSELs for Atomic Clocks

Darwin K. Serkland*[a], Gregory M. Peake[a], Kent M. Geib[a], Robert Lutwak[b], R. Michael Garvey[b], Mathew Varghese[c], Mark Mescher[c]

[a]Sandia National Laboratories, Albuquerque, NM 87185
[b]Symmetricom, Beverly, MA 01915
[c]Charles Stark Draper Laboratory, Cambridge, MA 02139

ABSTRACT

The spectroscopic technique of coherent population trapping (CPT) enables an all-optical interrogation of the ground-state hyperfine splitting of cesium (or rubidium), compared to the optical-microwave double resonance technique conventionally employed in atomic frequency standards. All-optical interrogation enables the reduction of the size and power consumption of an atomic clock by two orders of magnitude, and vertical-cavity surface-emitting lasers (VCSELs) are preferred optical sources due to their low power consumption and circular output beam. Several research teams are currently using VCSELs for DARPA's chip-scale atomic clock (CSAC) program with the goal of producing an atomic clock having a volume < 1 cm^3, a power consumption < 30 mW, and an instability (Allan deviation) < 1x10^-11 during a 1-hour averaging interval.

This paper describes the VCSEL requirements for CPT-based atomic clocks, which include single mode operation, single polarization operation, modulation bandwidth > 4 GHz, low power consumption (for the CSAC), narrow linewidth, and low relative intensity noise (RIN). A significant manufacturing challenge is to reproducibly obtain the required wavelength at the specified VCSEL operating temperature and drive current. Data are presented that show the advantage of operating at the D1 (rather than D2) resonance of the alkali atoms. Measurements of VCSEL linewidth will be discussed in particular, since atomic clock performance is especially sensitive to this parameter.

Keywords: VCSEL, vertical-cavity surface-emitting laser, atomic clock, spectroscopy, cesium, rubidium, linewidth, relative intensity noise, frequency standard

1. INTRODUCTION

In 2002, the Defense Advanced Research Projects Agency (DARPA) initiated a program to develop a Chip-Scale Atomic Clock (CSAC), which would enable high-accuracy timing in portable battery-powered devices. In particular, DARPA set a 4-year goal to produce a prototype atomic clock having a volume < 1 cm^3, a power consumption < 30 mW, and a fractional frequency instability (Allan deviation) < $1x10^{-11}$ during a 1-hour averaging interval. Such portable atomic clocks could be carried into locations where reception of Global Positioning System (GPS) signals is impaired and enable position information to be quickly and accurately determined by using the timing information from the atomic clock rather than from the GPS satellites. Moreover, if such clocks could be mass produced using micro-electronics fabrication techniques, the unit cost could be lowered to below $500, at which point such clocks could replace ovenized crystal oscillators in a large number of precision timing applications.

In 2000, the demonstration of an all-optical atomic clock using a modulated VCSEL[1] rather than an RF cavity paved the way to dramatically reduce the size and power consumption of atomic frequency standards. This paper will discuss the requirements of VCSELs used in atomic clocks. Since atomic clocks have relatively demanding requirements on VCSELs, compared to data communication applications, it is expected that such high-precision VCSELs will be more costly to produce. Depending on their cost, the potential market for small atomic clocks may rise to the order of 100,000 units per year. While this potential market is roughly 100 times smaller than the data communication VCSEL market, atomic clock manufacturers may be willing to pay 10 times the price of a data communication VCSEL, making it an economically viable market for VCSELs.

*DKSERKL(at)sandia.gov; phone: (505) 844-5355; fax: (505) 844-8985; http://www.sandia.gov

2. ATOMIC CLOCK PHYSICS

In this section we will discuss the essential physics of atomic clocks, with the goal of understanding the basis of the VCSEL requirements to be discussed in the following section. We start with a description of the conventional optical-microwave double resonance interrogation technique, as employed in conventional rubidium atomic clocks.[2] Then we will discuss the all-optical coherent population trapping (CPT) technique that enables smaller and lower-power atomic clocks using VCSELs.

Fig. 1(a) shows the relevant energy levels of the rubidium (Rb) atom. In particular, the $5S_{1/2}$ ground state is split into 2 sublevels, labeled a and b, due to the hyperfine interaction between the nuclear and electronic spins. The hyperfine splitting of the ground state of Rb is approximately 6.8 GHz. Because the two ground state sublevels a and b are metastable, the linewidth of the 6.8-GHz transition is narrow (<500 Hz), as indicated schematically in Fig. 1(b). At room temperature, the populations of sublevels a and b are approximately equal, since the 6.8-GHz hyperfine splitting is much less than kT/h = 6.3 THz (at T= 300 K). In a conventional commercial rubidium clock, shown schematically in Fig. 1(c), an ^{87}Rb gas discharge lamp emits both optical frequencies f_{ac} and f_{bc}. By a coincidence of nature, the ^{85}Rb isotope absorbs the f_{bc} light, transmitting the f_{ac} light to the ^{87}Rb cell inside the RF cavity. By the mechanism of optical pumping, the f_{ac} light depopulates level a, reducing the absorption of the f_{ac} light. When the RF cavity is excited at exactly the 6.8-GHz hyperfine splitting frequency, the microwave interaction repopulates level a, increasing the absorption of f_{ac} light. If the photocurrent generated by the photodiode (PD), shown in Fig. 1(c), is measured versus the RF excitation frequency, a response similar to that shown in Fig. 1(b) is obtained. Locking the RF frequency to the photocurrent dip at 6.8 GHz yields a precisely know frequency – the clock frequency. In a commercial Rb clock, the precise 6.8 GHz microwave source is synthesized from an RF oscillator, whose frequency is servoed to the atomic resonance, thereby providing a convenient user output at 10.0 MHz.

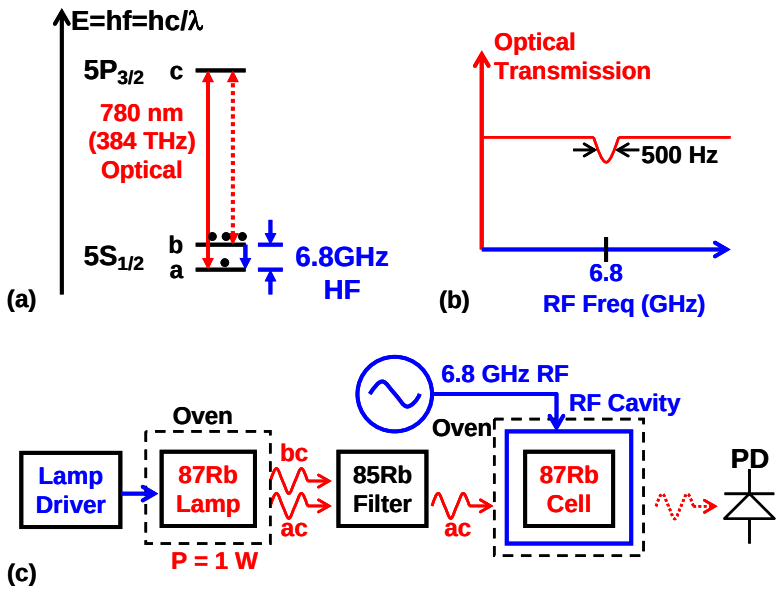

Fig. 1. Conventional double-resonance (optical and microwave) rubidium atomic clock physics. (a) Rubidium energy levels, showing the ground state 6.8-GHz hyperfine splitting and the optical 780-nm D2 transition. (b) Narrow (<500 Hz) clock transition resonance at 6.8 GHz. (c) Schematic of a typical commercial double-resonance rubidium atomic clock.

The conventional rubidium clock, shown schematically in Fig. 1(c), consumes approximately 10 W. Approximately 1 W is required to excite the ^{87}Rb gas discharge lamp, 1 W is required for microwave synthesis at 6.8 GHz, 1 W is required for the electronics, and the majority of the power is used to heat the ovens that stabilize the temperature of the ^{87}Rb gas discharge lamp and the ^{87}Rb cell and RF cavity. While a diode laser could replace the ^{87}Rb gas discharge lamp, thereby saving considerable power and volume, the 6.8-GHz RF cavity still necessitates a large volume and high power consumption.

Coherent population trapping (CPT) offers an alternative (all-optical) interrogation method that does not require a 6.8 GHz RF cavity around the rubidium gas cell.[3] Fig. 2(a) shows the relevant energy levels of the valence electron in a cesium (Cs) atom. Similar to rubidium, the $6S_{1/2}$ ground state of Cs is split into 2 sublevels, labeled a and b, due to the hyperfine interaction between the nuclear and electronic spins. The hyperfine splitting of the ground state of Cs is approximately 9.2 GHz. In fact, the internationally-accepted definition of the second is the time equal to exactly 9,192,631,770 oscillation periods of the cesium hyperfine frequency. Coherent population trapping requires the simultaneous application of 2 coherent optical frequencies f_{ac} and f_{bc}, such that the difference frequency exactly matches the 9.2-GHz ground state hyperfine splitting. A clever and convenient way to obtain 2 such frequencies is to modulate a VCSEL at 4.6 GHz with a small-amplitude sinusoidal waveform, thereby obtaining frequency modulation (FM) sidebands at ±4.6 GHz from the carrier optical frequency of 352 THz (852nm), as shown schematically in Fig. 2(c). Fig. 2(b) shows the required elements of a CPT atomic clock; namely, a 4.6-GHz microwave source to drive the VCSEL with approximately 0 dBm of power, a VCSEL with > 4 GHz FM modulation bandwidth tuned to exactly 852.4 nm (vacuum wavelength), a quarter-wave plate to create a pure circular polarization state, a cesium cell heated to approximately 80°C, and a low-frequency photodiode (PD) to measure transmission of the VCSEL light. If the 4.6-GHz FM modulated VCSEL is tuned by increasing its DC drive current, the transmitted optical power measured by the photodiode exhibits a 1-GHz-wide absorption dip, shown in Fig. 2(d), when the laser is tuned to the mid-point between the f_{ac} and f_{bc} frequencies, such that the first-order sidebands excite both the f_{ac} and f_{bc} transitions simultaneously.

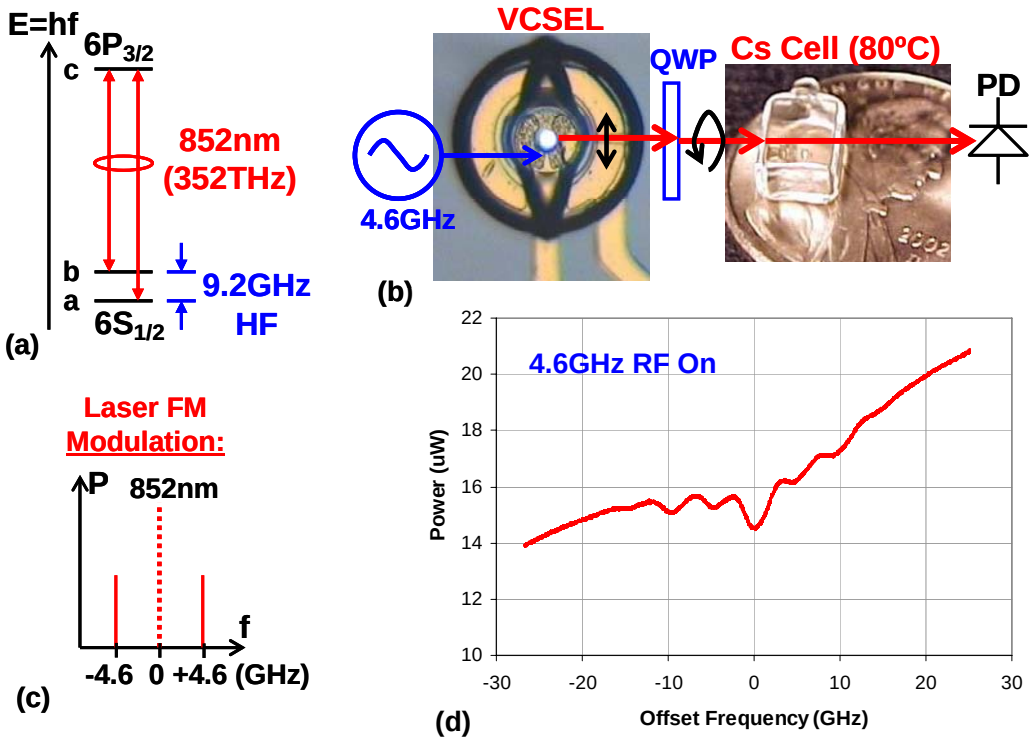

Fig. 2. Coherent population trapping (CPT) atomic clock physics. (a) Cesium energy levels, showing the ground state 9.2-GHz hyperfine level splitting and the optical 852-nm D2 transition. (b) Schematic of a typical CPT atomic clock. (c) Illustration of the first order sidebands at ±4.6 GHz created by frequency modulation of the VCSEL. (d) Detected power of the modulated VCSEL versus frequency offset. The VCSEL frequency was tuned over this small 50-GHz range by increasing its DC drive current by a small amount (0.4 mA).

Coherent population trapping (CPT) refers to the fact that a fraction of the cesium atoms become “trapped” in a coherent superposition of the ground states a and b, which does not absorb light due to destructive interference between the ac and bc transition probability amplitudes.[4,5] When the modulated VCSEL is tuned to the approximately 1-GHz-wide absorption resonance, and the modulation frequency is tuned in the vicinity of 4.6 GHz, a narrow (and small) increase in the transmitted optical power is observed at exactly half of the 9.2-GHz hyperfine frequency, as shown

schematically in Fig. 3. In an atomic clock application, the 4.6-GHz microwave source is locked to this narrow CPT resonance, yielding a frequency that is exactly half of the cesium ground state hyperfine splitting. A CPT frequency standard can also be made using rubidium (instead of cesium), in which case the microwave frequency is locked to the rubidium CPT resonance at 3.4-GHz.

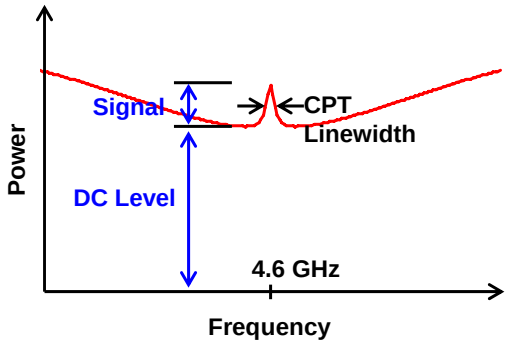

Fig. 3. Schematic illustration of the CPT resonance peak versus the RF frequency driving the VCSEL. The contrast is defined as η = Signal/(DC Level). The figure of merit is defined as $\xi=\eta Q$, where Q is the ratio of the RF resonance frequency to the CPT linewidth. Typically the contrast is on the order of 1% and the linewidth is on the order of 1 kHz.

For either Cs or Rb, there are two possible optically excited states "c" that can be employed, due to the fine structure (spin-orbit) splitting of the upper P-state. The two possible optical absorption wavelengths are called D1 and D2, corresponding to the $P_{1/2}$ and $P_{3/2}$ excited states, respectively. A more detailed energy level diagram for cesium is shown in Fig. 4(a). For cesium, the D1 transition occurs at 894.6 nm (vacuum wavelength) and the D2 transition occurs at 852.4 nm (vacuum wavelength). For rubidium, the D1 line is at 795.0 nm (vacuum wavelength) and the D2 line is at 780.2 nm (vacuum wavelength). For both rubidium[6] and cesium[7] it has been demonstrated that the CPT clock resonance figure of merit, defined in Fig. 3, is higher for the D1 transition. For this reason, the D1 wavelength is generally preferred over the D2 wavelength for atomic clocks. The figure or merit for D1 vs. D2 in cesium is shown in Fig. 4(b).

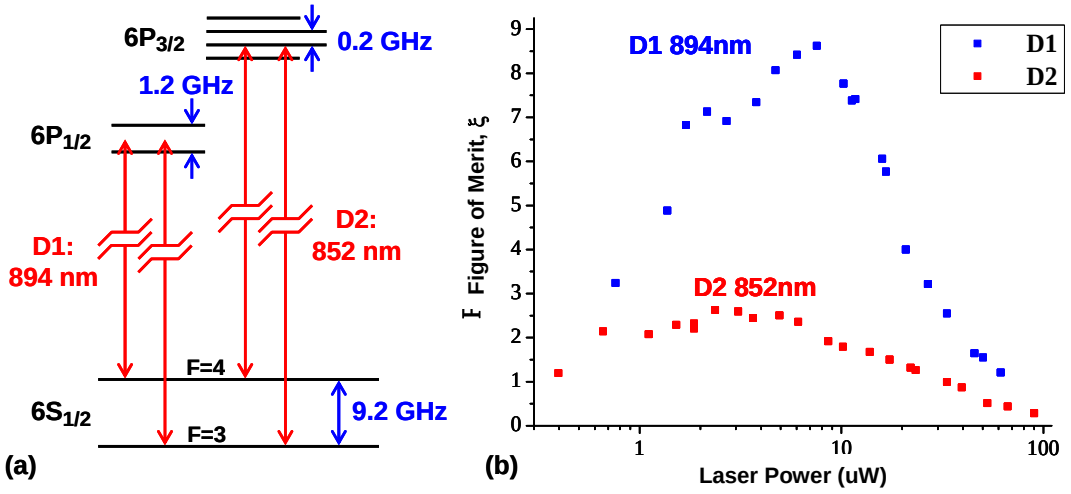

Fig. 4. (a) Cesium energy level diagram showing the fine-structure (spin-orbit) splitting, yielding $6P_{1/2}$ and $6P_{3/2}$ levels, corresponding to D1 and D2 optical transitions, respectively. The hyperfine (nuclear spin) splitting of all three levels is shown also. (b) Figure of merit versus laser power for the CPT clock resonance. The D1 wavelength is preferred for its higher figure of merit.

3. VCSEL REQUIREMENTS FOR ATOMIC CLOCKS

In this section we will describe the requirements for VCSELs to be used in CPT-based atomic clocks, as motivated by the atomic clock physics discussed in the previous section.

First, the VCSEL must operate at a single frequency that is tunable to exactly the D1 or D2 resonance wavelength of Cs or Rb. The relevant optical transition wavelengths (in vacuum) are for cesium 894.6 nm (D1) and 852.4 nm (D2), and for rubidium 795.0 nm (D1) and 780.2 nm (D2). The D1 transition wavelengths are generally preferred because they yield a higher figure of merit. If active cooling of the VCSEL is not possible, the operating temperature of the VCSEL must be chosen above the maximum ambient temperature at which the atomic clock is specified to operate. For example, if the atomic clock is specified to operate from 0 to 70°C, then the operating temperature of the VCSEL might be chosen at nominally 85°C. If the VCSEL temperature can only be varied within a ±5°C range, then the VCSEL wavelength must be accurate to within ±0.3 nm (assuming a typical VCSEL tuning coefficient of 0.06 nm/°C). Moreover, the VCSEL must operate in a single linear polarization so that a quarter-wave plate (QWP) can be used to produce a pure circular polarization in the alkali-atom gas cell. Circular polarization is required to enforce selection rules on the optical transitions (an explanation of the selection rules can be found in the references cited in the previous section). Perhaps most importantly, the VCSEL must operate at this precise wavelength in a stable single frequency and polarization mode for the life of the instrument, typically 10 years or longer.

The requirements for linear polarization, single frequency, and precise output wavelength at the prescribed operating temperature have significant implications for VCSEL device yield. In order to have a VCSEL yield above 90%, the typical example discussed above would require an epitaxial growth accuracy of ±0.15 nm and uniformity across the 3-inch GaAs wafer of ±0.15 nm. These requirements are approximately 10 times more demanding than typical accuracies obtained in the best epitaxial growth facilities. In addition, for oxide confined VCSELs, the oxide aperture diameter (typically about 3 μm for single transverse mode operation) must be controlled to within ±0.1 μm, since the wavelength also depends on the oxide aperture diameter. This requirement is approximately 2 times more demanding than the results that are achieved at the most reproducible fabrication facilities. Thus, it seems likely that production yields of VCSELs that meet the atomic clock wavelength requirements might be 10% or less, even with exceptionally accurate epitaxial growth and fabrication.

For low power consumption of the atomic clock, the VCSEL DC power consumption should be limited to 2 mW, which necessitates a threshold current below 1 mA. For many oxide-confined VCSELs this threshold current requirement is not difficult to meet. In order to create FM sidebands (at for example ±4.6 GHz), the VCSEL should have an FM modulation bandwidth above 4 GHz. This requirement is also motivated by the desire for low power consumption of the atomic clock, since ideally 0 dBm (1 mW) of RF power at 4.6 GHz should be sufficient to transfer most of the carrier frequency power into the sidebands at ±4.6 GHz. A key ingredient that enables efficient RF frequency modulation of the VCSEL is to provide approximate impedance matching of the VCSEL to the driving RF oscillator.

The final VCSEL requirement that we will discuss is the desire for a narrow linewidth (< 100 MHz). To understand the impact of VCSEL linewidth on clock performance, consider a VCSEL that is tuned to the center of the 1-GHz-wide absorption dip shown in Fig. 2(d). Any frequency noise present on the laser will be converted to amplitude noise due to the slope of the atomic transmission versus frequency curve, as shown schematically in Fig. 5. Amplitude noise on the transmitted light limits the ability to accurately determine the center of the CPT resonance peak and thus directly degrades the short-term stability of the atomic clock. In order to minimize amplitude noise on the transmitted optical signal, the laser linewidth (measured in a bandwidth comparable to the loop bandwidth of the atomic clock) should be less than 10% of the approximately 1-GHz-wide absorption dip. Due to the inherently short photon lifetime in a typical VCSEL cavity, achieving < 100 MHz linewidth is challenging. A typical VCSEL has a linewidth of a few hundred MHz, and the narrowest reported VCSEL linewidth is approximately 3 MHz.[8] It should also be mentioned that due to the strong dependence of VCSEL frequency on drive current (typically -125 MHz/μA), the current source that drives the VCSEL must be very stable to achieve a narrow linewidth.

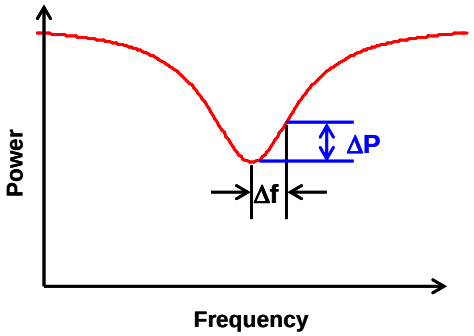

Fig. 5. Schematic illustration of the conversion of laser frequency noise to transmitted amplitude noise by the approximately 1-GHz-wide absorption line shape.

4. MINIATURE ATOMIC CLOCK USING AN 894-NM VCSEL

As an intermediate milestone in DARPA's CSAC program, the Symmetricom-Draper-Sandia team has produced a miniature atomic clock (MAC) with a volume < 10 cm^3 and a power consumption < 200 mW. An integrated VCSEL/detector chip was used in a double-pass cell transmission geometry, as shown in Fig. 6(a). The folded-optics geometry provides a relatively long cell transmission path in a small volume. The approximately 2-mm cubed cell is shown in Fig. 6(b) suspended from an octagon-shaped frame by several thin tethers that provide the thermal isolation necessary to minimize the heater power required to heat the cell to approximately 80°C.[9]

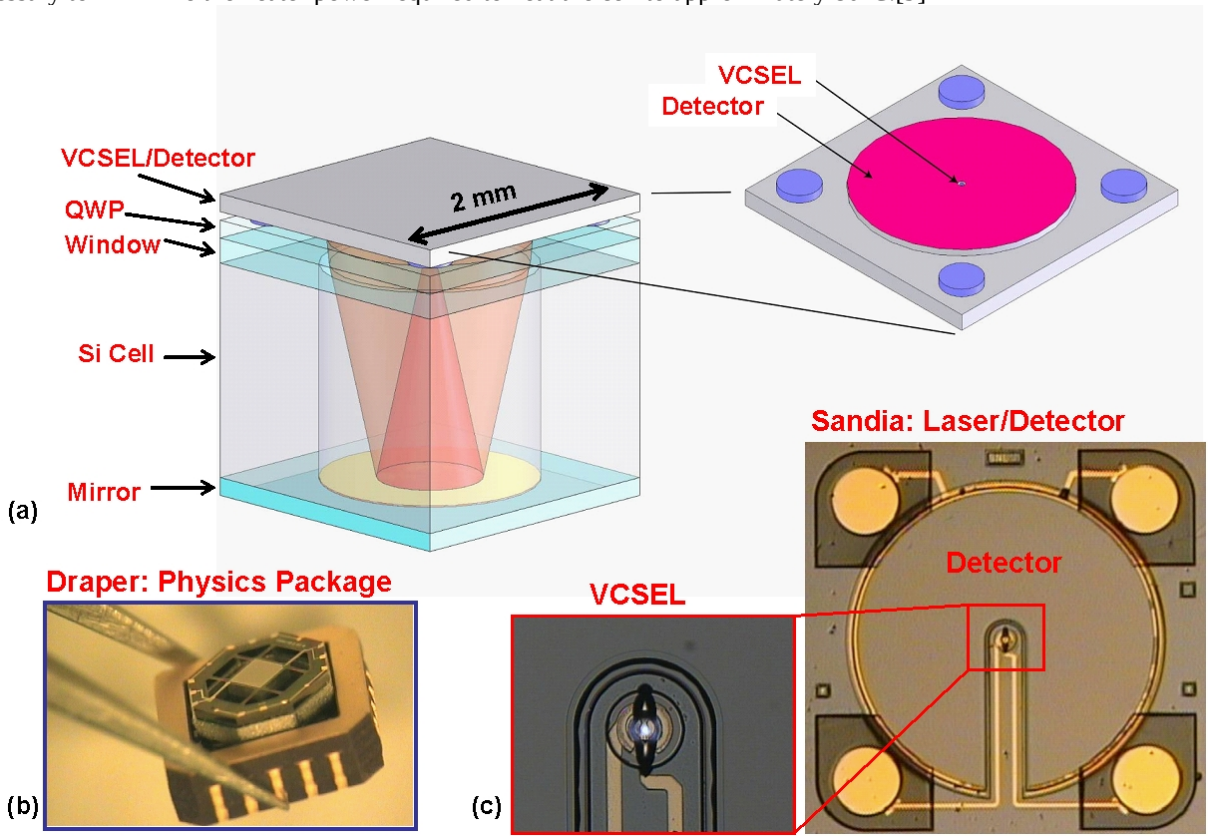

Fig. 6. (a) Conceptual illustration of the folded-optics physics package in which the VCSEL emits downward through a silicon cell containing Cs and a buffer gas. A reflective surface at the bottom of the cell reflects the diverging VCSEL light back toward the integrated photodiode that surrounds the VCSEL. (b) Photograph of the 2-mm cubed cell supported by 16 thin tethers inside of an octagon shaped frame. (c) Optical micrographs of the 2-mm square integrated VCSEL/detector chip.

A custom integrated VCSEL/RCPD (resonant-cavity photodiode) chip at 894 nm was designed and fabricated at Sandia in order to enable the folded-optics approach. A photograph of the 2-mm x 2-mm chip is shown in Fig. 6(c). The VCSEL is located at the center of the chip and is shown emitting light in the close-up view of Fig. 6(c). Surrounding the VCSEL is a 1.5-mm diameter RCPD. Electrical connections to the VCSEL and RCPD are provided by the four round flip-chip bond pads located at the corners of the chip.

As shown schematically in Fig. 7(a), the epitaxial semiconductor structure of the 894-nm VCSELs is grown on a semi-insulating GaAs substrate to minimize parasitic capacitances. The bottom distributed Bragg reflector (DBR) is designed as a high reflector, containing 36 pairs of n-doped quarter-wave high-index $Al_{0.16}Ga_{0.84}As$ and low-index $Al_{0.92}Ga_{0.08}As$ layers. The active region contains 5 undoped (intrinsic) $In_{0.07}Ga_{0.93}As$ quantum wells to provide optical gain near 890 nm. A quarter-wave layer of p-doped $Al_{0.98}Ga_{0.02}As$ immediately above the active region is selectively oxidized to form a circular oxide aperture that confines current to the center of the device.[10] The oxide aperture diameter is kept below 4 microns so that the VCSEL emits predominantly in the fundamental transverse mode. The top DBR is designed as an output coupling mirror, containing 25 pairs of p-doped quarter-wave low-index and high-index layers. The output power and voltage versus current data for a 3-micron-aperture VCSEL are shown in Fig. 8(a). Notice that the threshold is only 0.3 mA at 1.54 V, so that less than 1 mW of DC electrical power is required to operate the VCSEL. The VCSEL is optimized for single longitudinal and transverse mode operation with a linearly polarized output. The optical emission spectrum of the VCSEL at a drive current of 1.0 mA is shown in Fig. 8(b). The spectrum shows that the higher order transverse modes are suppressed by approximately 35 dB relative to the fundamental transverse mode.

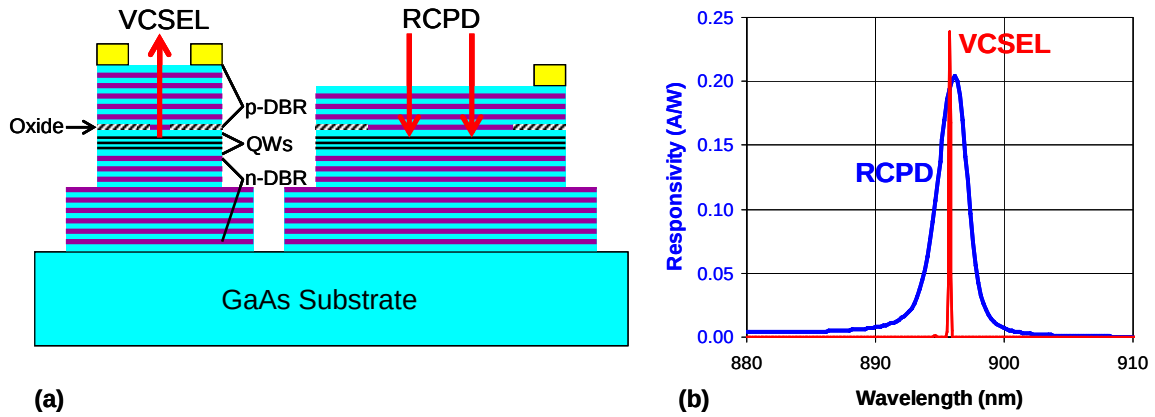

Fig. 7. (a) Cross sectional schematic of integrated VCSEL/RCPD device. The top of the RCPD region is etched to a depth of 0.25-wavelengths to spoil the Q of this region and thereby increase the responsivity and acceptance bandwidth. (b) RCPD responsivity versus wavelength shows a response peak of width 2.8 nm that is automatically matched to the VCSEL emission spectrum, also shown.

The resonant-cavity photodiode (RCPD) is fabricated using the same epitaxial material as the VCSEL, but part of the top DBR is etched away to improve the optical impedance match by reducing the top mirror reflectivity from 99.77% to 97.18%. The responsivity versus wavelength of a test RCPD device is shown in Fig. 7(b). The half-maximum-response bandwidth of the RCPD is 2.8 nm. The emission spectrum (on a linear scale) of a single-mode VCSEL located near the RCPD is superimposed on the responsivity plot in Fig. 7(b) to show the relative spectral alignment of the VCSEL and RCPD. Since the VCSEL and RCPD share the same epitaxial material, their nominal resonance wavelengths coincide and will track each other with changes in the ambient temperature. However, as suggested in Fig. 7(b), the VCSEL resonance wavelength is slightly blue shifted due the transverse optical confinement of the small oxide aperture.[11] Driving more current into the VCSEL will locally heat the laser and red-shift its emission wavelength into better alignment with the RCPD resonance.

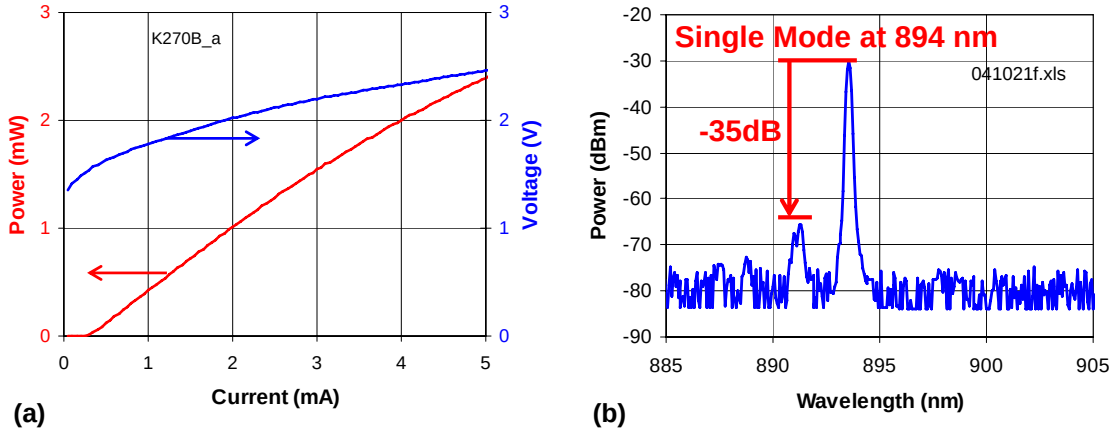

Fig. 8. (a) VCSEL output power and voltage versus current. The threshold current is 0.3 mA and the threshold voltage is 1.54 V. (b) VCSEL emission spectrum at 1 mA, showing > 35 dB of higher order transverse mode suppression.

In order to minimize power consumption, it is important that good impedance matching be provided between the 4.6-GHz microwave oscillator and the VCSEL so that microwave power is efficiently delivered to the laser. Fig. 9(a) shows the measured electrical reflection coefficient S_{11} of an 850-nm VCSEL from 0.1 to 20.1 GHz. As expected for a diode, the low frequency differential resistance decreases as the bias current is increased. The VCSEL equivalent circuit is shown in Fig. 9(b), for a bias current of 1 mA. This equivalent circuit was used to approximately impedance match the VCSEL to the microwave oscillator output, enabling adequate FM sidebands to be created with approximately 0 dBm (1 mW) of RF power.

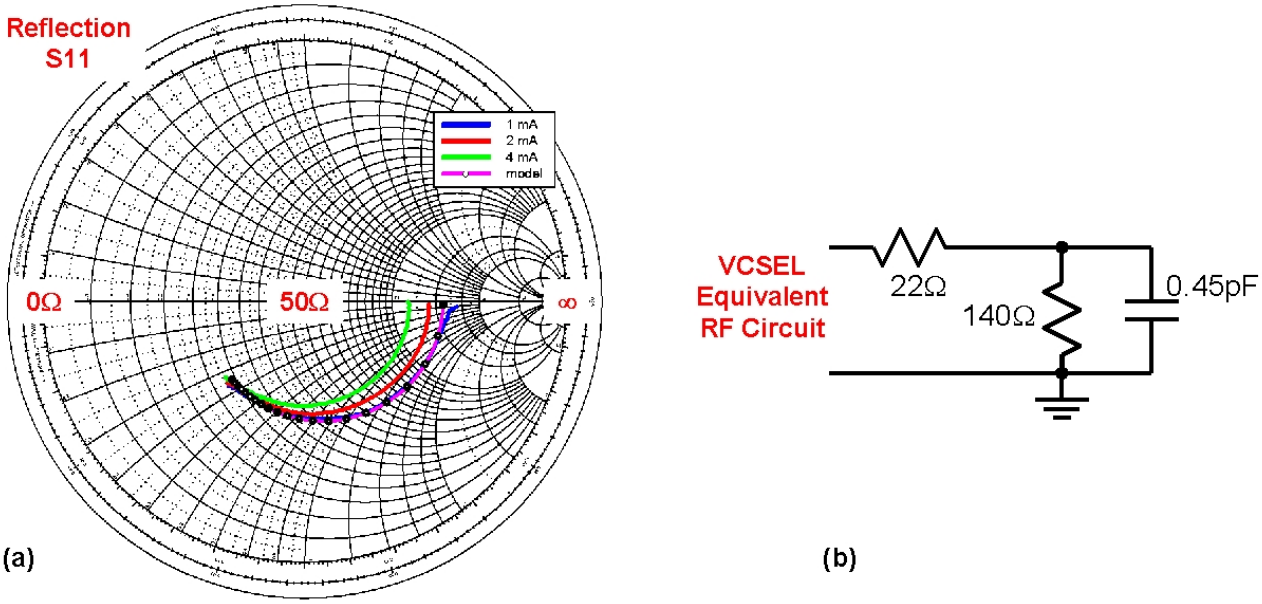

Fig. 9. (a) Electrical reflection S_{11} measurements on a VCSEL from 0.1 to 20.1 GHz. The dots show the 1-mA bias equivalent circuit S_{11} parameters at 1 GHz increments, starting at 0.1 GHz. (b) The VCSEL input equivalent circuit at 1 mA bias current.

As discussed in the previous section, good atomic clock stability requires a relatively narrow VCSEL linewidth. Fig. 10(a) shows a schematic of the optical heterodyne measurement setup that we employed to measure the linewidth of an 850-nm VCSEL. For this measurement, an external-cavity laser diode (EOSI, linewidth < 1 MHz) at 850-nm was tuned to a frequency f_1, approximately 1 GHz below the VCSEL frequency f_2. The two optical beams were combined using a 50% beam splitter and coupled into an 850-nm single-mode fiber and detected with a 12-GHz photoreceiver (New

Focus 1580-B) whose output was fed into an electrical spectrum analyzer. The spectrum analyzer resolution bandwidth was set at 2 MHz. The resulting beat note appeared at approximately 850 MHz, as shown in Fig. 10(b). A Lorentzian with a 50-MHz FWHM linewidth fits the data well. The VCSEL drive current for this measurement was 1.5 mA, which was supplied by a low-noise current source. Also, the VCSEL was temperature stabilized in an oven to minimize thermal frequency drifts during the measurement.

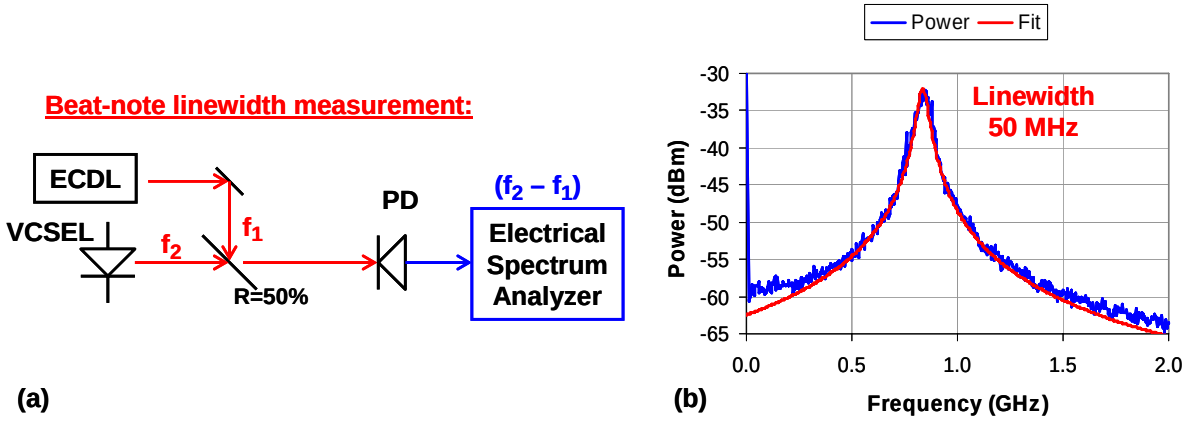

Fig. 10. (a) Schematic of the heterodyne setup for measuring VCSEL linewidth. (b) Representative VCSEL linewidth data, which is fitted closely with a 50-MHz-wide Lorentzian.

Fig. 11(a) shows the physics package from Fig. 6(b) mounted on a printed circuit board containing all of the atomic clock circuitry, including the 4.6-GHz microwave oscillator.[12] Control loops for cell temperature, VCSEL current, and oscillator frequency are simultaneously implemented on this circuit board, using a microprocessor and several A-to-D and D-to-A converters. The circuit board measures 35 mm by 39 mm. A mu-metal housing is placed around the circuit board, as shown in Fig. 11(b), in order to shield the atomic resonance cell from external magnetic fields. The mu-metal housing encloses a volume < 10 cm^3, and the operating power of the atomic clock is 155 mW.

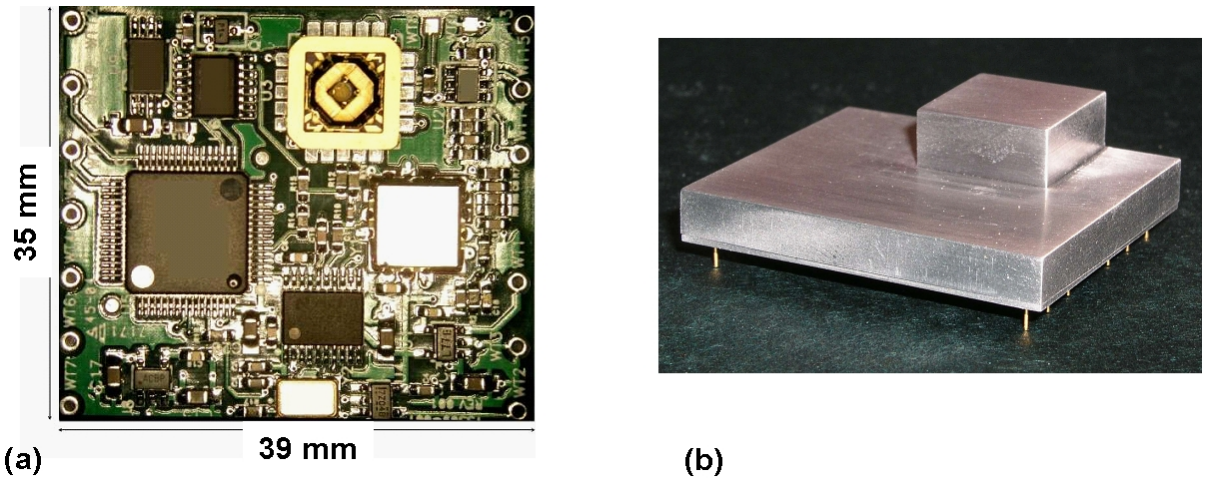

Fig. 11. (a) MAC printed circuit board containing the physics package (near the top), a 4.6-GHz voltage controlled oscillator, a phase locked loop, and microprocessor for controlling the cell temperature, the VCSEL current, and the oscillator frequency. (b) The MAC circuit board enclosed in a mu-metal magnetic shield housing having volume less than 10 cm^3.

Fig. 12 shows the Allan deviation of the relative offset frequency $y = (f_{meas} - f_0)/f_0$ versus the measurement time interval τ. The short term frequency stability of the MAC is approximately $\sigma_y = 4 \times 10^{-10}/\tau^{1/2}$, which surpasses the DARPA specification of $\sigma_y = 6 \times 10^{-10}/\tau^{1/2}$.

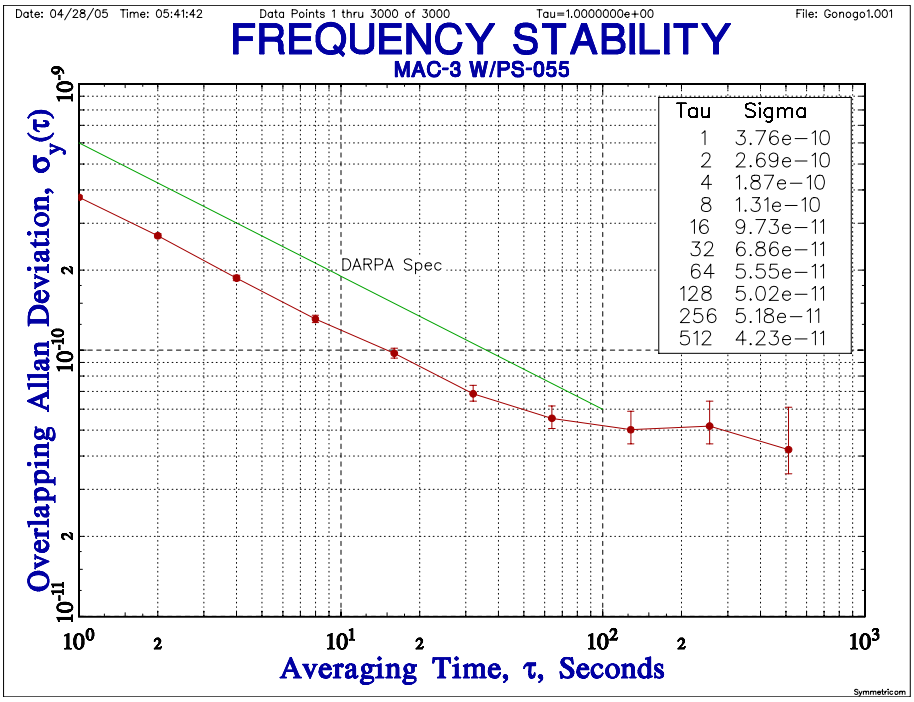

Fig. 12. Allan deviation of the MAC offset frequency $y = (f_{meas} - f_0)/f_0$ versus averaging time, showing that the MAC performance exceeds the DARPA requirement.

5. CONCLUSIONS

In conclusion, the coherent population trapping (CPT) technique enables small low-power optically interrogated atomic clocks. VCSELs are preferred optical sources due to their low power consumption, circular output beam, and high modulation bandwidth. The VCSEL must operate in a single frequency mode that is tunable to the atomic transition wavelength, preferably the rubidium D1 transition at 795.0 nm or the cesium D1 transition at 894.6 nm. This rigid wavelength constraint will likely result in a significant loss of yield during VCSEL production.

Other VCSEL requirements for atomic clocks include linearly polarized output, narrow linewidth (< 100 MHz), low power consumption (< 2 mW), high frequency modulation bandwidth (> 4 GHz), and impedance matching to the driving RF oscillator at 3.4 GHz (Rb) or 4.6 GHz (Cs). Achieving a narrow VCSEL linewidth is typically one of the more important challenges for optimum atomic clock performance. While the potential market for atomic clock VCSELs will probably not exceed 100,000 devices/year within the next 5 years, we believe that the market can support a high-volume VCSEL cost approximately 10 times that of a standard data communication VCSEL.

ACKNOWLEDGEMENT

The authors wish to thank G. A. Keeler, T. M. Bauer, T. W. Hargett, V. M. Montaño, and A. T. Ongstad for their expert technical assistance. This work was supported by Sandia, a multiprogram laboratory operated by Sandia Corporation, a Lockheed Martin Company, for the United States Department of Energy's National Nuclear Security Administration under contract DE-AC04-94AL85000.

REFERENCES

1. J. Kitching, S. Knappe, N. Vukicevic, L. Hollberg, R. Wynands, and W. Weidmann, "A Microwave Frequency Reference Based on VCSEL-Driven Dark Line Resonances in Cs Vapor," IEEE Trans. Instrum. Meas., vol. 49, pp. 1313–1317, 2000.
2. R. Lutwak, D. Emmons, W. Riley, and R.M. Garvey, "The Chip-Scale Atomic Clock – Coherent Population Trapping vs. Conventional Interrogation", Proceedings of the 34th Annual Precise Time and Time Interval (PTTI) Systems and Applications Meeting, December 3-5, 2002, Reston, VA, pp. 539-550.
3. N. Cyr, M. Tetu, and M. Breton, "All-optical microwave frequency standard: A proposal," IEEE Trans. Instrum. Meas., vol. 42, pp. 640–649, 1993.
4. J. Vanier, A. Godone, and F. Levi, "Coherent population trapping in cesium: Dark lines and coherent microwave emission," Phys. Rev. A, vol. 58, pp. 2345–2358, 1998.
5. Y.-Y. Jau, E. Miron, A. B. Post, N. N. Kuzma, and W. Happer, "Push-Pull Optical Pumping of Pure Superposition States", Phys. Rev. Lett., vol. 93, p. 160802-1, 2004.
6. M Stähler, R. Wynands, S. Knappe, J. Kitching, L. Hollberg, A. Taichenachev, and V. Yudin, "Coherent population trapping resonances in thermal 85Rb vapor: D1 vs D2 line excitation," Optics Letters, vol. 27, pp. 1472-1474, 2002.
7. R. Lutwak, D. Emmons, T. English, W. Riley, A. Duwel, M. Varghese, D. K. Serkland, and G. M. Peake, "The Chip-Scale Atomic Clock – Recent Development Progress", Proceedings of the 35th Annual Precise Time and Time Interval (PTTI) Systems and Applications Meeting, December 2-4, 2003, San Diego, CA, pp. 467-478.
8. F. Monti di Sopra, H. P. Zappe, M. Moser, R. H¨ovel, H.-P. Gauggel, and K. Gulden, "Near-Infrared Vertical-Cavity Surface-Emitting Lasers with 3-MHz Linewidth", IEEE Photon. Technol. Lett., vol. 11, pp. 1533-1535, 1999.
9. R. Lutwak, J. Deng, W. Riley, M. Varghese, J. Leblanc, G. Tepolt, M. Mescher, D.K. Serkland, K.M. Geib, and G.M. Peake, "The Chip-Scale Atomic Clock – Low-Power Physics Package", Proceedings of the 36th Annual Precise Time and Time Interval (PTTI) Systems and Applications Meeting, December 7-9, 2004, Washington, DC, pp. 339-354.
10. D. L. Huffaker, D. G. Deppe, K. Kumar, and T. J. Rogers, "Native-oxide defined ring contact for low threshold vertical-cavity lasers,"Appl. Phys. Lett., vol. 65, p. 97, 1994.
11. D. K. Serkland, G. R. Hadley, K. D. Choquette, K. M. Geib, and A. A. Allerman, "Modal frequencies of vertical-cavity lasers determined by an effective-index model," Appl. Phys. Lett., vol. 77, pp. 22-24, 2000.
12. R. Lutwak, P. Vlitas, M. Varghese, M. Mescher, D.K. Serkland, and G.M. Peake, "The MAC – A Miniature Atomic Clock", Proceedings 2005 Joint IEEE International Frequency Control Symposium and Precise Time and Time Interval (PTTI) Systems and Applications Meeting, Vancouver, BC, August 29-31, 2005, in print.